Jiménez-García, Lidia; Higueras, María Ángeles; Herranz, Sandra; Hernández-López, Marta; Luque, Alfonso; Las Heras, Beatriz de; Hortelano, Sonsoles. **A hispanolone-derived diterpenoid inhibits M2-Macrophage polarization in vitro via JAK/STAT and attenuates chitin induced inflammation in vivo**. Biochem Pharmacol. 2018 Aug:154:373-383.

https://doi.org/10.1016/j.bcp.2018.06.002

A hispanolone-derived diterpenoid inhibits M2-Macrophage polarization *in vitro* via JAK/STAT and attenuates chitin induced inflammation *in vivo*.

Lidia Jiménez-García[a,#], María Ángeles Higueras[a,#], Sandra Herranz[a], Marta Hernández-López[b], Alfonso Luque[a], Beatriz de las Heras[b,*] and Sonsoles Hortelano[a,*]

[a]Unidad de Terapias Farmacológicas. Área de Genética Humana. Instituto de Investigación de Enfermedades Raras (IIER), Instituto de Salud Carlos III, Madrid, Spain. [b]Departamento de Farmacología. Facultad de Farmacia, Universidad Complutense de Madrid (UCM), Madrid, Spain.

#L Jiménez-García and MA Higueras have equally contributed to this work.

*B de las Heras and S Hortelano are both corresponding authors.

- Lidia Jiménez-García, ljimenez@isciii.es
- María Ángeles Higueras, mhigueras@isciii.es
- Sandra Herranz, sherranz@isciii.es
- Marta Hernández López, izzara_899@hotmail.com
- Alfonso Luque, aluque@isciii.es
- Beatriz de las Heras, lasheras@ucm.es
- Sonsoles Hortelano, shortelano@isciii.es

Address correspondence to:

Sonsoles Hortelano. Unidad de Terapias Farmacológicas. Área de Genética Humana. Instituto de Investigación de Enfermedades Raras (IIER), Instituto de Salud Carlos III, Ctra Majadahonda-Pozuelo, Km 2,200. 28220 Majadahonda, Madrid, Spain.

e-mail: shortelano@isciii.es. Phone: (34) 918223291; Fax: (34) 918223269

Abstract

Macrophages are highly plastic cells that adopt different functional phenotypes in response to environmental signals. Classically activated macrophages (M1) exhibit a pro-inflammatory role, mediating host defense against microorganisms or tumor cells; whereas alternatively activated macrophages (M2) perform a range of physiological processes, including inflammation, wound repair and tissue remodeling. Interestingly, M2 macrophages have been involved in pathological settings such as tumor progression, parasitic infection and respiratory disorders. Consequently, the search of new agents able to control macrophage polarization is on the basis of new therapeutic strategies.

In the present study, we have evaluated the effect of the hispanolone derivative 8,9-dehydrohispanolone-15,16-lactol (DHHL) on M2 macrophage polarization. Our results reveal that DHHL significantly inhibited IL-4- or IL-13-stimulated M2 macrophage activation, as showed by reduced expression of M2 markers. In addition, DHHL suppressed IL-4-induced STAT-6 and JAK-1 tyrosine phosphorylation, suggesting that this compound inhibited M2 polarization by suppressing the JAK-STAT signaling pathway. Finally, DHHL prevented eosinophil recruitment and the presence of F4/80$^+$-CD206$^+$ M2-like macrophages in an *in vivo* model of M2 polarization via administration of chitin. Collectively, these results confirm DHHL as a novel regulator of macrophage polarization suitable to design future therapies towards M2-macrophages mediated pathologies.

Key words: hispanolone, diterpenoids, macrophage polarization, STAT-6, chitin.

1. Introduction

Macrophages represent an essential cell population of innate immunity with a critical role in inflammation and host defense as well as in the maintenance of tissue homeostasis [1]. Two major phenotypes have been characterized: the classically activated macrophages (M1) and the alternatively activated macrophages (M2) [1;2]. These macrophages display a differential expression profile of cytokines, enzymes and cell-surface markers. M1 phenotype is driven by interferon-γ (IFN-γ), bacterial products, such as lipopolysaccharide (LPS), and Toll-like receptor (TLR) agonists. M1 macrophages exhibit antimicrobial and cytotoxic functions and are characterized by enhanced production of pro-inflammatory cytokines, expression of MHC class II molecules and generation of free radicals including nitric oxide (NO). Thus, M1 macrophages constitute a critical cellular component involved in the inflammatory response and antitumor immunity. Conversely, M2 macrophages differentiate in the presence of interleukin-4 (IL-4) or IL-13 cytokines and display anti-inflammatory and pro-tumorigenic activities by producing anti-inflammatory factors [IL-10, transforming growth factor-β (TGF-β), and IL-1 receptor antagonist], promoting angiogenesis, tissue remodeling and tissue repair [1;3;4]. In addition, M2 macrophages express a different subset of innate immunity molecules as compared to M1 macrophages [2;3;5]. Expression of IL-10 cytokine, arginase-1 (Arg-1), mannose receptor (MRC1/CD206) and genes associated with tissue remodelling such as chitinase 3-like 3 (Ym-1) and Found in Inflammatory Zone 1 (Fizz-1), distinguish M2 macrophages from the other phenotype [2;6].

Molecularly, IL-4 and IL-13 bind to two types of transmembrane receptors named: type I, heterodimer formed by IL-4Rα and IL-4R common γ-chain, and type II, heterodimer formed by IL-4Rα and IL-13Rα1 chain. IL-4 signals through both receptors, whereas IL-13 stimulates exclusively the type II receptor. Type I receptors interact with JAK1 and JAK3 and downstream signal through two independent pathways: one mediated by STAT6 and the other by IRS-1/2-PI3K [3;7;8]. Furthermore, it has been described that IL-4Rα associates with JAK1 whereas IL-4RγC associates exclusively with JAK3. On the other hand, type II receptors interact with JAK1 and JAK2 and only signal through STAT6 [3;7-10]. Once STAT6 is phosphorylated by a member of the JAK family, it translocates into the nucleus and binds to specific promoters of target genes [2]. Relevant to our work, type I receptor is mainly expressed by hematopoietic cells [11].

An imbalance between M1-M2 macrophage populations has been reported in the context of various diseases. Development of chronic diseases including cancer, respiratory pathologies as chronic obstructive pulmonary disease (COPD), and the rare diseases idiopathic pulmonary fibrosis and cystic fibrosis, have been associated with an excessive accumulation of M2 macrophages [12;13]. Therefore, modulation of M1-M2 polarization may provide a novel therapeutic strategy to these diseases.

Natural products are one of the most successful sources of drug leads. Among them, the labdane diterpenoid hispanolone and its derivatives have been described to exert anti-inflammatory and anti-tumoral activities. We have previously reported that selected hispanolone derivatives reduced the release of inflammatory mediators as NO, prostaglandins and TNF-α in LPS-activated macrophages through inhibition of NF-κB [14]. In addition, they also exhibited *in vivo* anti-inflammatory effects in the mouse ear edema induced by 12-*O*-Tetradecanoylphorbol-13-acetate (TPA) model with inhibition and reduction of neutrophil infiltration [14]. However, the effects of these hispanolone derivatives on M2 macrophage polarization have not been reported. In the present study, we examined the role of the hispanolone derivative 8,9-dehydrohispanolone-15,16-

lactol (DHHL) on M2 macrophage polarization. Our results demonstrate that DHHL inhibited IL-4-induced expression of typical M2 markers as Arg-1, Fizz-1, Ym-1, MRC1, interferon regulatory factor-4 (IRF-4), or macrophage galactose N-acetyl-acetyl-galactosamine 2 (MGL-2) in a dose-dependent manner. Consistently, protein levels of Arg-1 and Ym-1 were reduced after DHHL treatment. In addition, DHHL significantly suppressed IL-4-induced JAK-STAT activation on macrophages, suggesting that JAK-STAT pathway might be involved in the inhibitory effects of DHHL on M2 polarization. Finally, the inhibitory effect of DHHL was also observed after stimulation with IL-13 and confirmed in an *in vivo* model of M2 polarization via administration of chitin. These data indicate that DHHL suppresses macrophage alternative phenotype induced by a M2-like environment,

2. Materials and methods

2.1. Animals.

All animal care and experimental procedures were conducted in accordance with the guidelines for Animal Care and were approved by the Instructional Animal Care and Use Committee (IACUC) of the Instituto de Salud Carlos III. Studies involving animals are reported in accordance with the ARRIVE guidelines for reporting experiments involving animals [15;16]. Studies were performed on C57BL/6J mice. Mice were housed four per cage in a controlled environment (12 hour light/dark cycle at 21°C) with free access to water and food.

2.2. Materials.

8,9-dehydrohispanolone-15,16-lactol (DHHL) was obtained as previously described [14]. Stocks were dissolved in dimethyl sulfoxide (DMSO) and subsequently diluted in PBS before use (maximum concentration 0.01%).

2.3. Cell culture and preparation of elicited peritoneal macrophages.

Peritoneal macrophages were elicited by intraperitoneal injection of 2.5 ml 3% thioglycollate (Becton-Dickinson) in distilled water and were prepared as reported by Través et al. [17]. Cells were seeded at 1 x 10^6/cm^2 in RPMI containing 10% FBS. Nonadherent cells were removed 2 hours after seeding by extensive washing with medium.

Cells were pre-treated with DHHL or appropriate control for 15 minutes at 37ºC before addition of 20 ng/ml of IL-4/IL-13 (Peprotech) for the indicated times.

2.4. MTT assay for cell viability.

Cells were incubated in the presence of different concentrations of DHHL for 24 h. MTT (3-[4,5-dimethylthiazol-2-yl]-2,5-diphenyl tetrazolium bromide) (2 mg/ml) was added to the wells and incubated for 3 h at 37 ºC. The reaction product, formazan, was extracted with DMSO and the absorbance was read at 540 nm as previously reported [18]. Assays were performed in triplicate, and results are expressed as the percent reduction in cell viability compared to untreated control cultures for at least three independent experiments.

2.5. Arginase activity measurement.

Arginase activity was assessed in cell lysates indirectly by measuring urea concentration generated by the arginase-dependent hydrolysis of L-arginine [19]. Briefly, cells were lysed with 20 mM Tris (pH 7.5), 150 mM NaCl, 2mM EDTA, and 0.1% Triton X-100–containing protease inhibitor mixture (Sigma) for 30 minutes at room temperature. Standards were prepared by serially diluting a stock of urea (Sigma) in 50 mM Tris-HCl (pH 7.5) to yield a standard range from 25 to 1,500 µg/ml. Lysates and standards (25 µl) were mixed with 25 µl of 10 mM $MnCl_2$ in 50 mM Tris-HCl (pH 7.5) in a 2 ml Eppendorf tube. Tubes were then incubated for 10 minutes at 55°C for activation. Next, arginine hydrolysis was conducted by incubating 50 µl of the lysates and standards with 50 µl of 0.5 M L-arginine at 37°C for 75 minutes, followed by the addition of 400 µl stopping solution ($H_2SO_4/H_3PO_4/H_2O$ = 1/3/7, v/v/v). To measure the amount of urea in each tube, 50 µl of 9% 1-phenyl-1,2-propanedione-2-oxime (Sigma) in 100% ethanol was added to each sample and standard, and tubes were incubated at 100°C for 60 minutes. Tubes were placed in the dark at 25°C for 30 minutes. Samples and standards (100 µl/well) were transferred in triplicate to a 96-well plate, and optical density was read at 540 nm with a 690 nm correction. Sample concentrations were determined from the standard curve and converted to Arginase Units using the following formula: [Urea Produced (µg/ml)/Total Protein (µg/ml)].

2.6. Total protein extracts and Western blot.

Cells cultured in 6-well plates were lysed at 4ºC with 0.2 ml buffer A per well (0.5% Chaps, 10mM Tris pH 7.5, 1mM Cl_2Mg, 1mM EGTA, 10% Glycerol, 5mM β-mercaptoethanol) and protease inhibitor cocktail (Sigma). Protein content was assayed with the Bio-Rad protein reagent. All cell fractionation steps were carried out at 4°C. Protein extracts were subjected to SDS-PAGE (10-15% gels) and blotted onto polyvinylidene difluoride membranes (GE Healthcare), which were incubated with the following antibodies: anti-Arg-1 (sc-20150), anti-p-STAT-6 (sc-71793), anti-STAT-6 (sc-374021), anti-p-JAK-1 (sc-101716) (Santa Cruz Biotechnology), anti-Ym-1 (Stem Cell) or anti-β-actin (Sigma). After incubation with HRP-conjugated secondary antibody, protein bands were revealed with an enhanced chemiluminescence kit (GE Healthcare). β-actin was used as a loading control. After treatment with 100 mM β-mercaptoethanol, 2% SDS in TBS and heating at 60ºC for 30 minutes, blots were sequentially re-probed with different antibodies.

2.7. RNA isolation and quantitative PCR.

Total RNA was isolated from cells with Trizol reagent (Invitrogen). Quantitative PCR (SYBR Green) analysis was performed with an ABI 7500 Fast sequence analyser as described [17]. Each sample was run in duplicate, and all samples were analyzed in parallel for the expression of the housekeeping gene 36B4 (acidic ribosomal phosphoprotein P0), which was used as an endogenous control for normalization of the expression level of target genes. Fold induction was determined from mean replicate values. Primer used for quantitative PCR sequences are shown in Table 1.

2.8. *In vivo* chitin-induced M2 macrophages polarization model.

Intranasal or intraperitoneal (i.p.) administration of chitin particles results in activation of macrophages with a M2 phenotype [20;21]. For *in vivo* experiments, C57BL/6J mice were divided in four experimental groups: control, DHHL, chitin, chitin + DHHL (n=5 per group).

Intraperitoneal administration of chitin: Chitin (800ng, Sigma) was injected i.p. to induce recruitment and polarization of M2 cells into the peritoneum, as previously described [22]. One hour after administration of chitin, mice were i.p. injected with 2 mg/kg body weight (b.w.) DHHL in 1 ml sterile saline. Peritoneal exudate cells (PECs) were collected by lavage after 48 hours and gene induction was determined by quantitative PCR. Additionally, PECs were analyzed by standard techniques of flow cytometry (MACSQuant, Miltenyi Biotec) to detect macrophages (F4/80$^+$-CD11b$^+$), eosinophils (SiglecF$^+$-CD11b$^+$) or M2 macrophages (F4/80$^+$-CD206$^+$).

Intranasal administration of chitin: Mice were anesthetized via i.p. injection with a mixture of ketamine/xilacin (1mg/ml). The anesthetized mouse was then subjected to intranasal inhalation of PBS, DHHL (30μg) and/or chitin (200 ng). DHHL and chitin particles were suspended at indicated concentrations in 30μl PBS and administered by placing dropwise in both nasal orifices of the mouse. After 48 h of chitin administration, mice were sacrificed and tissue samples and broncoalveolar lavage were obtained as described below.

2.9. Analysis of cell populations by flow cytometry.

Peritoneal exudate single-cell suspensions were preincubated with FcγR-specific blocking mAb (2.4G2) (BD Bioscience) for 30 min at 4ºC, and washed before labeling. Cells were incubated with the following antibodies AlexaFluor 647-anti-F4/80 (Abcam), PE-SiglecF (BD Pharmingen), Alexa Fluor 488-anti-CD206 (BioLegend), Alexa Fluor 488-anti-CD11b (BD Pharmingen). Samples were examined on a MACSQuant (Miltenyi Biotec) flow cytometer and data were analyzed with the MACSQuantify software.

2.10. Histology and immunohistochemistry of lung tissues.

For histological analysis, lungs were removed and fixed in 10% neutral buffered formalin at 4°C for 24 h. Tissues were embedded in paraffin, sectioned at 5 μm thickness, and stained with hematoxylin and eosin (H&E) to evaluate organ morphology and inflammatory foci using a light microscope.

For immunostaining, tissue sections were deparaffinized and subjected to standard antigen retrieval process by boiling into sodium-citrate buffer (0.1 M Na citrate, 0.1 M citric acid, pH 6.0), followed by 3% H_2O_2 incubation for 10 min, and blocking with 1.5% normal horse serum for 2 h. Samples were incubated overnight at 4 °C with control rabbit IgG or rabbit polyclonal antibody to Ym-1 (1:500, Stem Cell Technologies) diluted in blocking buffer. Sections were then washed and incubated at room temperature for 30 min with biotinylated secondary antibody followed by the Vectastain Elite ABC kit (Vector Labs). A DAB Peroxidase Substrate Kit (Vector Labs) was used to visualize peroxidase reaction. The number of Ym-1$^+$ macrophages was quantified microscopically for each slide from 5-10 randomly chosen fields of five independent mice, as previously described [23].

2.11. Broncoalveolar lavage (BAL).

Animals were euthanized by an overdose of isofluorane and BAL was performed after exposing the trachea with a midline neck incision and doing a tracheostomy with a 14-gauge needle. Ice-cold sterile PBS was introduced (1 ml, 3 times); about 80% of the volume was recovered each time. The BAL fluid was centrifuged (5000 rpm, 5 min, 4°C) and cell pellets were collected for the analysis of M2 markers by quantitative PCR.

2.12. Analysis of the lung cellular infiltrate.

Lungs were excised and digested with 0.1% collagenase in HBSS for 1 hour at 37º. Lung cell suspensions were filtrated through 70 µm filters and resuspended in free serum medium. Macrophages, eosinophils, or M2 macrophages cell counts were performed by flow cytometry (MACSQuant, Miltenyi Biotec).

2.13. Measurement of cytokine production.

IL-4 and IL-13 cytokines released to BAL fluid after 48 h chitin administration were determined by ELISA kits (R&D Systems) following manufacturer´s recommendation. Absorbance values were converted to the concentration of each cytokine in the BAL fluid (picograms per milliliter) by interpolation to the respective standard curve.

2.14. Statistical analysis.

Data presented are shown as means ± SD of at least three independent experiments. Statistical significance was estimated by Student's *t* test for comparison between two groups. For comparison between two or more groups, one-way ANOVA, followed by Bonferroni’s post hoc comparisons was used. Differences were considered significant at

$*p < 0.05$. All statistical analyses were conducted using GraphPad Prism 5.0 (GraphPad Software).

3. Results

3.1. DHHL inhibits the expression of IL-4-induced M2 markers.

The chemical structure of DHHL is shown in Fig. 1A. In order to discard toxicity of DHHL on peritoneal macrophages, cells were treated for 24 h with a range of DHHL concentrations from 1 to 25 μM and cell viability was measured by MTT assay. No significant effects on cell viability were observed after DHHL treatment (Fig. 1B). A classical readout for M2 macrophage polarization is the induction of Arg-1. To explore the potential effects of DHHL on Arg-1 activation, we examined the levels of this gene after IL-4 treatment by quantitative PCR. As shown in Fig. 1C, mRNA levels of Arg-1 were markedly increased upon IL-4 treatment, whereas DHHL pre-incubation inhibited Arg-1 expression in a dose-dependent manner. In concordance, a significant decrease in arginase activity, using an urea-based assay, was also observed in peritoneal macrophages after DHHL treatment (Fig. 1D). Furthermore, regulation of Arg-1 was also analyzed using a specific Arg-1 antibody. DHHL significantly suppressed IL-4-induced Arg-1 expression (Fig. 1E).

In addition to Arg-1, other well established M2 markers as Fizz-1, Ym-1, MRC1, IRF-4, or MGL-2 have been described to be upregulated in M2 macrophages [5]. As observed for Arg-1 expression, DHHL treatment significantly inhibited IL-4-stimulated M2-type markers expression in a dose-dependent manner (Fig. 2A). Inhibitory effects were confirmed by western blot with a dose-dependent inhibition of Ym-1 protein levels in macrophages treated with IL-4 (Fig. 2B).

3.2. DHHL prevents IL-13-stimulated M2 macrophage polarization.

In order to examine whether the inhibitory effect of DHHL could be extended to other M2 stimuli, we induced M2 polarization of macrophages with IL-13. We found that DHHL treatment potently inhibited expression of all M2 markers evaluated above in a similar manner as previously observed for IL-4 treatment (Fig. 3A). In addition, protein levels of Arg-1 and Ym-1 were also reduced in the presence of DHHL (Fig. 3B). Thus, DHHL acts as a broad inhibitor of alternative macrophage polarization elicited by different M2-like stimuli.

3.3. DHHL suppresses IL-4–mediated JAK-1/STAT-6 activation.

Alternative macrophage activation has been described to be mainly regulated by an IL-4Rα–STAT6–dependent mechanism [3]. We next evaluated STAT-6 activity after IL-4 stimulation in the presence or absence of DHHL. As shown in Fig. 4A, IL-4 stimulation induced a robust STAT-6 phosphorylation with maximal activation at 60 and 90 minutes. By contrast, in the presence of DHHL, a marked inhibition of STAT-6 activation was observed at all time points analyzed. The ability of DHHL to suppress IL-4-induced STAT-6 phosphorylation indicates that this compound might interfere with the upstream signaling components such as JAK-1. Analysis of tyrosine phosphorylation of JAK-1 after DHHL treatment showed attenuation of IL-4–induced JAK-1 activation (Fig.4B). Therefore, DHHL may modulate M2 polarization of macrophages through inhibition of JAK/STAT-6 signaling pathways.

3.4. DHHL inhibits M2 polarized macrophages in a chitin challenged *in vivo* model.

It has been reported that chitin challenge recruits M2 macrophages to the site of administration, being a critical event for subsequent recruitment of eosinophils [20;21;24;25]. To corroborate our *in vitro* results, the *in vivo* effects of DHHL were investigated using this model.

First, we evaluated the effect of DHHL after i.p. administration of chitin. Analysis of the different cell populations present in peritoneal exudate from chitin-challenged mice in the presence or absence of DHHL was performed by flow cytometry. The number of chitin-elicited whole macrophage population (F4/80$^+$-CD11b$^+$), M2 macrophages subset (F4/80$^+$-CD206$^+$) and eosinophils (SiglecF$^+$-CD11b$^+$) was severely impaired in mice treated with DHHL (Fig. 5A,B). Furthermore, expression of M2 genes (Arg-1, Fizz-1, and Ym-1) was markedly lower in PECs from chitin-challenged mice treated with DHHL compared to controls (Fig. 5C).

We next evaluated the effect of DHHL on allergic inflammation after intranasal administration of chitin. Analysis of the composition of lung cellular infiltrate by flow cytometry showed that exposure to chitin increased the number of macrophages (total and M2) and eosinophils; whereas the percentages of all these cell subsets were significantly lower after DHHL treatment (Fig. 6A). H&E histological analysis revealed that chitin challenge resulted in the increase of inflammatory cell infiltrates. In contrast, treatment with DHHL elicited protection against all these pathological features as evidenced by reduced cellular infiltration. Interestingly, lung sections from mice treated with DHHL alone exhibited normal lung morphology (Fig. 6B). Furthermore, Ym-1 expression was significantly reduced in lung tissues after DHHL treatment compared with the levels observed in chitin-elicited animals (Fig. 6C and D). Finally, in agreement with the protective effects observed in lung tissues, quantitative PCR analyses of BAL from the different groups demonstrated that treatment with DHHL significantly decreased the expression of typical M2 markers (Arg-1 and Ym-1) (Fig. 6E), supporting the inhibitory role of DHHL on M2 polarization.

Accumulation of eosinophils after chitin treatment has been described to contribute to the release of IL-4 and IL-13 [21]. In order to correlate the amounts of IL-4 or IL-13 released by chitin to the ability of gathering M2 polarized cells, we evaluated BAL samples for the effects of DHHL on both mRNA expression and cytokine levels after chitin administration. DHHL treatment reduced significantly chitin-induced gene expression and protein release of both cytokines (Fig. 7). All these results indicate that DHHL is an effective inhibitor of allergic inflammation.

4. Discussion

Macrophages display heterogeneous phenotypes ranging from pro-inflammatory M1 activation to anti-inflammatory M2 responses depending on the surrounding microenvironment. Interestingly, M1/M2 imbalances are critical in the development of various diseases. Accumulation of M2 macrophages has been described to contribute to chronic infections, fibrosis, allergy, and cancer [12;13]. Therefore, macrophage polarization from M2 to M1 or viceversa represents an attractive target in the search for new therapeutic strategies.

The labdane diterpenoid hispanolone was first isolated from *Ballota hispanica*, a Labiatae species growing in Spain and has been used as a leading compound for therapeutic purposes [26]. Hispanolone derivatives have been found to have excellent anti-inflammatory and anti-tumoral activities [14;18;27]. In this regard, hispanolone derivatives including DHHL have been shown profound effects on inflammation, exhibiting *in vivo* anti-inflammatory activity and reducing the production of inflammatory cytokines and mediators, as NO, through inhibition of NF-κB on LPS-activated macrophages [14]. Furthermore, we also reported the antitumoral effects of some derivatives by activating apoptotic cell death machinery and sensitizing tumor cells to TRAIL-induced apoptosis [18]. However, the effects of the hispanolone derivative DHHL on M2 macrophage polarization have not been described. In this work, we have investigated the effects of DHHL on M2 macrophage polarization, with particular focus on the JAK/STAT signaling pathway. Our results clearly show that DHHL inhibits macrophage polarization towards M2 phenotype *in vitro* and *in vivo*. DHHL reduced, in a dose-dependent manner, the expression of M2 markers (Arg-1, Fizz-1, Ym-1, MRC1, IRF-4 and MGL-2) induced by both IL-4 and IL-13 cytokines in murine peritoneal macrophages. Moreover, using an *in vivo* model of M2 polarization driven by chitin administration, we confirmed that DHHL inhibits alternative macrophage activation with a remarkable reduction in the expression of typical M2 markers (Arg-1, Fizz-1, and Ym-1).

Chitin is a widespread biopolymer of *N*-acetyl-β-D-glucosamine and a structural component of helminths, arthropods and fungi [28]. This biopolymer contributes to the development of allergic type 2 inflammation and parasitic worm immunity by enhancing the generation of alternatively activated macrophages [21]. Chitin challenge also recruits macrophages showing the M2 phenotype to the site of administration, being a critical event for subsequent recruitment of eosinophils [20;21;24;25]. In this scenario, we observed that administration of DHHL to chitin-challenged mice inhibited the recruitment of macrophages and eosinophils, diminished the expression of M2-associated genes (Arg-1 or Ym-1), and cytokines (IL-4 and IL-13) and reduced inflammatory cell infiltration in lung tissues. Moreover, flow cytometry analysis of lung macrophage subsets reconfirmed reduction of M2 macrophage population.

Up-regulation of Arg-1 expression has been described in sub-mucosal inflammatory cells of patients with asthma, as well as in the lungs of allergen-sensitized and challenged mice [29;30]. Moreover, the member of the murine chitinase family Ym-1 has been found to be highly induced during alternative macrophage activation in addition to Arg-1 [31]. Ym-1 plays an important role in Th2-biased immune responses such as helminth infections, airway inflammation, tissue remodeling and fibrosis [32], being also involved in experimental and clinical asthma [33]. Therefore, the M2-type inhibitory activity exerted by DHHL via reduction of Arg-1 and Ym-1 suggests that this compound may have therapeutical advantages for pathologies characterized by an exacerbated Th2 response. These versatile effects on macrophage polarization are similar to those described for other labdanes as andrographolide, which inhibited M1 or M2 polarization stages of macrophages depending on the biological status of these cells [34;35]. Furthermore, in line with our observations, a non-cytotoxic analogue of andrographolide also exerted protective roles in a murine model of allergic inflammation [7].

Our data showed that DHHL suppresses tyrosine phosphorylation of STAT-6 and the up-stream kinase JAK-1, suggesting that the most likely mechanism by which DHHL inhibits M2 activation is via modulation of JAK-1/STAT-6 pathway (Fig. 8). Indeed, these results are in agreement with those reported in the literature where alternative macrophage activation has been described to be mainly regulated by an IL-4Rα-STAT6-dependent mechanism [3]. Other natural compounds also interfere with the JAK/STAT pathway. In this regard, as constitutive activation of STAT-3 occurs frequently in cancer cells, numerous studies have been mainly focused on the inhibitory effects of terpenoids on the JAK/STAT-3 pathway. For example, andrographolide down-regulated the expression of MRC1 in IL-4 induced macrophages via regulation of ERK 1/2 and AKT pathways [35]; whereas triterpenoids such as corosolic acid and oleanolic acid [36-38], and dihydroxycoumarins as esculetin and daphnetin [39], inhibited macrophage polarization to M2 phenotype by suppressing STAT-3 activation. Nevertheless, to the best of our knowledge, this is the first report of the inhibitory effects of labdane diterpenoids on the JAK-1/STAT-6 pathway.

Although the mechanism responsible for such activity requires further research, the finding that DHHL contains two Michael acceptor functional groups (α,β-unsaturated carbonyl groups) suggests that this diterpenoid may react with critical cysteines in target proteins. In this regard, hispanolone derivatives have been previously described to inhibit IKK activation via this mechanism [14]. In addition, synthetic oleanane triterpenoids that can also confer Michael addition with nucleophilic targets, have been described to block JAK-1/STAT-3 activation via interaction with cysteine residues in the JAK-1 kinase domain [40].

In summary, our data show that DHHL is a potent modulator of macrophage polarization, being the JAK-1/STAT-6 signaling pathway involved in the regulation towards the M2 phenotype by this compound. From this perspective, DHHL might be a promising drug candidate for the treatment of human pathologies characterized by exacerbated M2 macrophage activation.

Conflict of interest.

B. de las Heras and S. Hortelano are inventors on a Spanish patent application on labdane diterpenoids as anti-tumoral agents. The other authors declared no conflict of interest.

Acknowledgements.

This study was supported by grant PI11/00036, PI14/00055 and PI17/00012 from the FIS, MPY 1410/09 from ISCIII and Spanish Ministry of Health (Instituto de Salud Carlos III; RD12/0036/0059) to S. Hortelano, and by grant IERPY 1149/16 to AL. L J-G was supported by FIS (FI12/00340). S Herranz was supported by IERPY 1149/16 from ISCIII.

Figure legends

Figure 1. Effects of DHHL on IL-4-induced Arg-1 expression. (A) Chemical structure of DHHL. (B) Peritoneal macrophages were incubated with the indicated concentrations of DHHL for 24 h. Cell viability was determined by MTT assay. (C) Peritoneal macrophages were preincubated with the indicated concentrations of DHHL for 15 minutes, following by stimulation with IL-4 (20ng/ml) for 6 hours**.** Arg-1 expression was determined by quantitative PCR. (D) Peritoneal macrophages were preincubated with the indicated concentrations of DHHL for 15 minutes, following by stimulation with IL-4 (20ng/ml) for 24 hours. Arg-1 activity was evaluated by urea production. (E) Protein levels of Arg-1 were evaluated by Western blot after stimulation of peritoneal macrophages as in D. Bands intensities were analyzed by densitometry, normalized to β-actin and represented as the mean ± SD from three independent experiments. Gene expression was represented as mean ± SD mRNA fold induction with respect to the control condition (n=3). *p<0.05, and **p<0.01 with respect to IL-4 treatment in C, D and E.

Figure 2. DHHL inhibited M2-type markers expression induced by IL-4 treatment. (A) Peritoneal macrophages were preincubated with the indicated concentrations of DHHL for 15 minutes, following by stimulation with IL-4 (20ng/ml) for 6 hours**.** Fizz-1, Ym-1, MRC1, IRF-4 and MGL-2 expression was determined by quantitative PCR. (B) Peritoneal macrophages were preincubated with the indicated concentrations of DHHL for 15 minutes, following by stimulation with IL-4 (20ng/ml) for 24 hours**.** Protein levels of Ym-1 were evaluated by Western blot. Bands intensities were analyzed by densitometry, normalized to β-actin and represented as the mean ± SD from three independent experiments. Gene expression was represented as mean ± SD mRNA fold

induction with respect to the control condition (n=3). *p<0.05, and **p<0.01 with respect to IL-4 treatment in A and B.

Figure 3. DHHL inhibited M2-type markers expression induced by IL-13 treatment. (A) Peritoneal macrophages were preincubated with the indicated concentrations of DHHL for 15 minutes, following by stimulation with IL-13 (20ng/ml) for 6 hours**.** Arg-1, Fizz-1, Ym-1, MRC1, IRF-4 and MGL-2 expression was determined by quantitative PCR. (B) Peritoneal macrophages were preincubated with the indicated concentrations of DHHL for 15 minutes, following by stimulation with IL-13 (20ng/ml) for 24 hours**.** Protein levels of Arg-1 and Ym-1 were evaluated by Western blot. Bands intensities were analyzed by densitometry, normalized to β-actin and represented as the mean ± SD from three independent experiments. Gene expression was represented as mean ± SD mRNA fold induction with respect to the control condition (n=3). *p<0.05, and **p<0.01 with respect to IL-13 treatment in A and B.

Figure 4. DHHL inhibited IL-4 induced phosphorylation of JAK-1/STAT-6. Peritoneal macrophages were preincubated with DHHL (10µM) for 15 minutes, following by stimulation with IL-4 (20ng/ml) for different times (15, 30, 60, 90, 120 minutes). (A) Phosphorylated levels of STAT-6 or (B) JAK-1 were evaluated by Western Blot. Bands intensities were analyzed by densitometry, normalized to β-actin and represented as the mean ± SD of the fold change from control condition (n=3). *p<0.05 with respect to IL-4 treatment.

Figure 5. DHHL impaired M2 macrophage polarization *in vivo* after i.p. administration of chitin. C57BL/6J mice were divided in four experimental groups: control (PBS), DHHL, chitin, chitin + DHHL (n=5 per group). C57BL/6J mice were subjected to 2mg DHHL per kilogram body weight (b.w.) by i.p. injection in 1 ml sterile

saline one hour after administration of chitin (800 ng, i.p.). Peritoneal exudate cells (PECs) were collected by lavage after 48 hours treatment and analyzed (A,B) by standard techniques of flow cytometry to detect macrophages (F4/80$^+$-CD11b$^+$), eosinophils (SiglecF$^+$-CD11b$^+$) or M2 macrophages (F4/80$^+$-CD206$^+$), or (C) by quantitative PCR to identify gene induction of M2-associated genes. A, Flow cytometry plots show cell population from a representative individual of each experimental condition. B, Cell quantification analyzed by flow cytometry. Dots represent values from individual mice. *p<0.05, and **p<0.01 with respect to chitin condition.

Figure 6. Effects of DHHL on lung inflammation and M2 polarization *in vivo.* Mice were anesthetized via i.p. injection with a mixture of ketamine/xilacin (1mg/ml) and subjected to intranasal inhalation with PBS, DHHL (30μg) and/or chitin (200 ng) as previously described. Lungs were evaluated after 48 hours treatment. (A) Analysis of lung cell populations was performed by flow cytometry. (B) Representative H&E lung histology from the different groups. Lower panels correspond to higher magnification of the inset traced in the upper panels. Asterisks indicate inflammatory cell infiltrates. (C) Representative immunohistochemistries of lung tissues labelled with Ym-1. Lower panels correspond to higher magnification of the inset traced in the upper panels. Arrows indicate Ym-1 positive cells. Scale bars are represented in each case. D) Quantification of Ym-1$^+$ cells. Cells were counted blindly in 5–10 randomly chosen fields and data are means ± S.D. of three independent lung sections from 5 mice. (E) Quantitative PCR was performed to determine changes on M2 marker expression on BALs obtained from the different groups. Dots represent values from individual mice. Data indicate mean ± SD of three independent experiments. *p<0.05, and **p<0.01 with respect to chitin condition.

Figure 7. Effects of DHHL on IL-4 and IL-13 release. Mice were anesthetized via i.p. injection with a mixture of ketamine/xilacin (1mg/ml) and subjected to intranasal inhalation with PBS, DHHL (30μg) and/or chitin (200 ng) as previously described. BALs were obtained after 48 hours treatment. BAL fluid was centrifuged and used for cytokine determination, whereas cell pellets were collected for the analysis of IL-4 and IL-13 mRNA by quantitative PCR. (A) Quantitative PCR was performed to determine changes on IL-4 and IL-13 expression on BALs collected from the different groups. (B) IL-4 and IL-13 protein levels were determined by ELISA. Dots represent values from individual mice. *p<0.05, and **p<0.01 with respect to chitin condition.

Figure 8. Proposed model for DHHL inhibition of alternatively activated macrophages polarization on M2-dependent environment

IL-4 and IL-13 signal through two different types of receptors, the type I (heterodimer constituted by IL-4Rα and IL-4R common γ-chain) or the type II (heterodimer formed by IL-4Rα and IL-13Rα1 chain). Type I receptors interact with JAK1 and JAK3, leading to activation of STAT6, and/or IRS-1/2 and PI3K. Type II receptors interact with JAK1 and JAK2 and signal through STAT-6. Activated STAT-6 induces the expression of genes related to the M2 phenotype (Arg-1, Ym-1, Fizz-1, MRC1, IRF-4, MGL-2). DHHL inhibits tyrosine phosphorylation of JAK-1, suppressing STAT-6 activation and inhibiting M2 macrophage polarization.

References

[1] F.O. Martinez, A. Sica, A. Mantovani, M. Locati, Macrophage activation and polarization, Front Biosci. 13 (2008) 453-61.

[2] F.O. Martinez, L. Helming, S. Gordon, Alternative activation of macrophages: an immunologic functional perspective, Annu. Rev. Immunol. 27 (2009) 451-83.

[3] S. Gordon, Alternative activation of macrophages, Nat. Rev. Immunol. 3 (2003) 23-35.

[4] D.M. Mosser and J.P. Edwards, Exploring the full spectrum of macrophage activation, Nat. Rev. Immunol. 8 (2008) 958-69.

[5] F.O. Martinez, L. Helming, R. Milde, A. Varin, B.N. Melgert, C. Draijer, B. Thomas, M. Fabbri, A. Crawshaw, L.P. Ho, N.H. Ten Hacken, J. Cobos, V, N.A. Kootstra, J. Hamann, D.R. Greaves, M. Locati, A. Mantovani, S. Gordon, Genetic programs expressed in resting and IL-4 alternatively activated mouse and human macrophages: similarities and differences, Blood 121 (2013) e57-e69.

[6] G. Raes, P. De Baetselier, W. Noel, A. Beschin, F. Brombacher, G. Hassanzadeh, Differential expression of FIZZ1 and Ym1 in alternatively versus classically activated macrophages, J. Leukoc. Biol. 71 (2002) 597-602.

[7] S.P. Guan, L.R. Kong, C. Cheng, J.C.W. Lim, W.S.F. Wong, Protective Role of 14-Deoxy-11,12-didehydroandrographolide, a Noncytotoxic Analogue of Andrographolide, in Allergic Airway Inflammation, J. Nat. Prod. 74 (2011) 1484-90.

[8] A.E. Kelly-Welch, E.M. Hanson, M.R. Boothby, A.D. Keegan, Interleukin-4 and interleukin-13 signaling connections maps, Science 300 (2003) 1527-8.

[9] S.J. Van Dyken and R.M. Locksley, Interleukin-4- and interleukin-13-mediated alternatively activated macrophages: roles in homeostasis and disease, Annu. Rev Immunol. 31 (2013) 317-43.

[10] A. Sica and A. Mantovani, Macrophage plasticity and polarization: in vivo veritas, J Clin Invest 122 (2012) 787-95.

[11] S. Gordon and F.O. Martinez, Alternative activation of macrophages: mechanism and functions, Immunity. 32 (2010) 593-604.

[12] C.E. Boorsma, C. Draijer, B.N. Melgert, Macrophage Heterogeneity in Respiratory Diseases, Mediators Inflamm. 2013 (2013) 769214.

[13] C.D. Mills, M1 and M2 Macrophages: Oracles of Health and Disease, Crit. Rev. Immunol. 32 (2012) 463-88.

[14] N. Giron, P.G. Traves, B.n. Rodriguez, R. Lopez-Fontal, L. Bosca, S. Hortelano, B. de las Heras, Supression of inflammatory responses by labdane-type diterpenoids, Toxicol. Appl. Pharmacol. 228 (2008) 179-89.

[15] C. Kilkenny, W. Browne, I.C. Cuthill, M. Emerson, D.G. Altman, Animal research: Reporting in vivo experiments: The ARRIVE guidelines, Br J Pharmacol 160 (2010) 1577-9.

[16] J.C. McGrath, G.B. Drummond, E.M. McLachlan, C. Kilkenny, C.L. Wainwright, Guidelines for reporting experiments involving animals: the ARRIVE guidelines, British Journal of Pharmacology 160 (2010) 1573-6.

[17] P.G. Traves, R. Lopez-Fontal, A. Luque, S. Hortelano, The tumor suppressor ARF regulates innate immune responses in mice, J. Immunol. 187 (2011) 6527-38.

[18] A. Mota, L. Jimenez-Garcia, S. Herranz, de Las Heras B., S. Hortelano, alpha-Hispanolol sensitizes hepatocellular carcinoma cells to TRAIL-induced apoptosis via death receptor up-regulation, Toxicol Appl. Pharmacol. 286 (2015) 168-77.

[19] S. Herranz, P.G. Traves, A. Luque, S. Hortelano, Role of the tumor suppressor ARF in macrophage polarization: Enhancement of the M2 phenotype in ARF-deficient mice, Oncoimmunol 1 (2012) 1227-38.

[20] T. Satoh, O. Takeuchi, A. Vandenbon, K. Yasuda, Y. Tanaka, Y. Kumagai, T. Miyake, K. Matsushita, T. Okazaki, T. Saitoh, K. Honma, T. Matsuyama, K. Yui, T. Tsujimura, D.M. Standley, K. Nakanishi, K. Nakai, S. Akira, The Jmjd3-Irf4 axis regulates M2 macrophage polarization and host responses against helminth infection, Nat. Immunol. 11 (2010) 936-44.

[21] T.A. Reese, H.E. Liang, A.M. Tager, A.D. Luster, N. Van Rooijen, D. Voehringer, R.M. Locksley, Chitin induces accumulation in tissue of innate immune cells associated with allergy, Nature 447 (2007) 92-6.

[22] L. Jimenez-Garcia, S. Herranz, A. Luque, S. Hortelano, Critical role of p38 MAPK in IL-4-induced alternative activation of peritoneal macrophages, Eur. J. Immunol. 45 (2015) 273-86.

[23] L. Jimenez-Garcia, S. Herranz, M.A. Higueras, A. Luque, S. Hortelano, Tumor suppressor ARF regulates tissue microenvironment and tumor growth through modulation of macrophage polarization, Oncotarget 7 (2016) 66835-50.

[24] V. Byles, A.J. Covarrubias, I. Ben-Sahra, D.W. Lamming, D.M. Sabatini, B.D. Manning, T. Horng, The TSC-mTOR pathway regulates macrophage polarization, Nat. Commun. 4 (2013) 2834.

[25] R.M. Roy, M. Wuthrich, B.S. Klein, Chitin elicits CCL2 from airway epithelial cells and induces CCR2-dependent innate allergic inflammation in the lung, J Immunol 189 (2012) 2545-52.

[26] G. Savona, F. Piozzi, B. Rodriguez, Hispanolone, a new furanoditerpene., Heterocycles 9 (1978) 257-61.

[27] P.G. Traves, R. Lopez-Fontal, I. Cuadrado, A. Luque, L. Bosca, de Las Heras B., S. Hortelano, Critical role of the death receptor pathway in the antitumoral effects induced by hispanolone derivatives, Oncogene 32 (2013) 259-68.

[28] S.M. Bowman and S.J. Free, The structure and synthesis of the fungal cell wall, BioEssays 28 (2006) 799-808.

[29] N. Zimmermann, N.E. King, J. Laporte, M. Yang, A. Mishra, S.M. Pope, E.E. Muntel, D.P. Witte, A.A. Pegg, P.S. Foster, Q. Hamid, M.E. Rothenberg, Dissection of experimental asthma with DNA microarray analysis identifies arginase in asthma pathogenesis, J Clin Invest 11 (2003) 1863-74.

[30] M.L. North, N. Khanna, P.A. Marsden, H. Grasemann, J.A. Scott, Functionally important role for arginase 1 in the airway hyperresponsiveness of asthma, Am J Physiol Lung Cell Mol Physiol 296 (2009) L911-L920.

[31] H.M. Jin, N.G. Copeland, D.J. Gilbert, N.A. Jenkins, R.B. Kirkpatrick, M. Rosenberg, Genetic Characterization of the Murine Ym1 Gene and Identification of a Cluster of Highly Homologous Genes, Genomics 54 (1998) 316-22.

[32] C.G. Lee, Chitin, Chitinases and Chitinase-like Proteins in Allergic Inflammation and Tissue Remodeling, Yonsei Med J 50 (2009) 22-30.

[33] G.L. Chupp, C.G. Lee, N. Jarjour, Shim Y.M., Holm C.T., He S., Dziura J.D., J. Reed, Coyle A.J., P. Kiener, M. Cullen, M. Grandsaigne, Dombret M.C., M. Aubier, M. Pretolani, J.A. Elias, A chitinase-like protein in the lung and circulation of patients with severe asthma, N Engl J Med 357 (2007) 2016-27.

[34] J.C.W. Lim, T.K. Chan, D.S. Ng, S.R. Sagineedu, J. Stanslas, W.F. Wong, Andrographolide and its analogues: versatile bioactive molecules for combating inflammation and cancer, Clinical and Experimental Pharmacology and Physiology 39 (2012) 300-10.

[35] W. Wang, J. Wang, S.f. Dong, C.h. Liu, P. Italiani, S.h. Sun, J. Xu, D. Boraschi, S.p. Ma, D. Qu, Immunomodulatory activity of andrographolide on macrophage activation and specific antibody response, Acta Pharmacol Sin 31 (2010) 191-201.

[36] Y. Fujiwara, M. Takeya, Y. Komohara, A Novel Strategy for Inducing the Antitumor Effects of Triterpenoid Compounds: Blocking the Protumoral Functions of Tumor-Associated Macrophages via STAT3 Inhibition, Biomed. Res. Int. 2014 (2014) 348539.

[37] Y. Fujiwara, Y. Komohara, R. Kudo, K. Tsurushima, K. Ohnishi, T. Ikeda, M. Takeya, Oleanolic acid inhibits macrophage differentiation into the M2 phenotype and glioblastoma cell proliferation by suppressing the activation of STAT3, Oncol. Rep. 26 (2011) 1533-7.

[38] Y. Fujiwara, Y. Komohara, T. Ikeda, M. Takeya, Corosolic acid inhibits glioblastoma cell proliferation by suppressing the activation of signal transducer and activator of transcription-3 and nuclear factor-kappa B in tumor cells and tumor-associated macrophages, Cancer Sci. 102 (2011) 206-11.

[39] Y. Kimura and M. Sumiyoshi, Antitumor and antimetastatic actions of dihydroxycoumarins (esculetin or fraxetin) through the inhibition of M2 macrophage differentiation in tumor-associated macrophages and/or G1 arrest in tumor cells, Eur. J. Pharmacol. 746 (2015) 115-25.

[40] R. Ahmad, D. Raina, C. Meyer, D. Kufe, Triterpenoid CDDO-Methyl Ester Inhibits the Janus-Activated Kinase-1 (JAK1)-signal Transducer and Activator of Transcription-3 (STAT3) Pathway by Direct Inhibition of JAK1 and STAT3, Cancer Res. 68 (2008) 2920-6.

Table

Table 1. List of primers used in Q-PCR experiments

Gene name	Primer 5’-3’
Arg-1	(F) 5´-TGAGAGACCACGGGGACCTG-3´, (R) 5´- GCACCACACTGACTCTTCCATTC-3´
Fizz-1	(F) 5´-CCATAGAGAGATTATCGTGGA-3´ (R) 5´-TGGTCGAGTCAACGAGTAAG-3´
Ym-1	(F) 5´-TGGAATTGGTGCCCCTACAA-3´ (R) 5´-AACTTGCACTGTGTATATTG-3´
MRC-1	(F) 5´-GTAGTACCGGAGGGTGCAGA-3´ (R) 5´-TTTGCATCAGTGAAGGTGGA-3´
IRF-4	(F) 5´-TGTGCTCTGAACAAGAGCAAT-3’ (R) 5´-TATGAACCTGCTGGGCTGG-3´
MGL-2	(F) 5´-AGCGGGAAGAGAAAAACCAG-3´ (R) 5´-ACCAGTAGCAGGAGGCTGAG-3´
IL-4	(F) 5´-ACCTGAGAACAGCGGAGGC-3´ (R) 5´-TCGGAAAACAGGTTCTCAGTGAG-3´
IL-13	(F) 5´-GGATATTGCATGGCCTCTGTAAC-3´ (R) 5´-AACAGTTGCTTTGTGTAGCTGA-3´
36B4	(F) 5´-AGATGCAGCAGATCCGCAT-3´ (R) 5´-GTTCTTGCCCATCAGCACC-3´

Figure 1

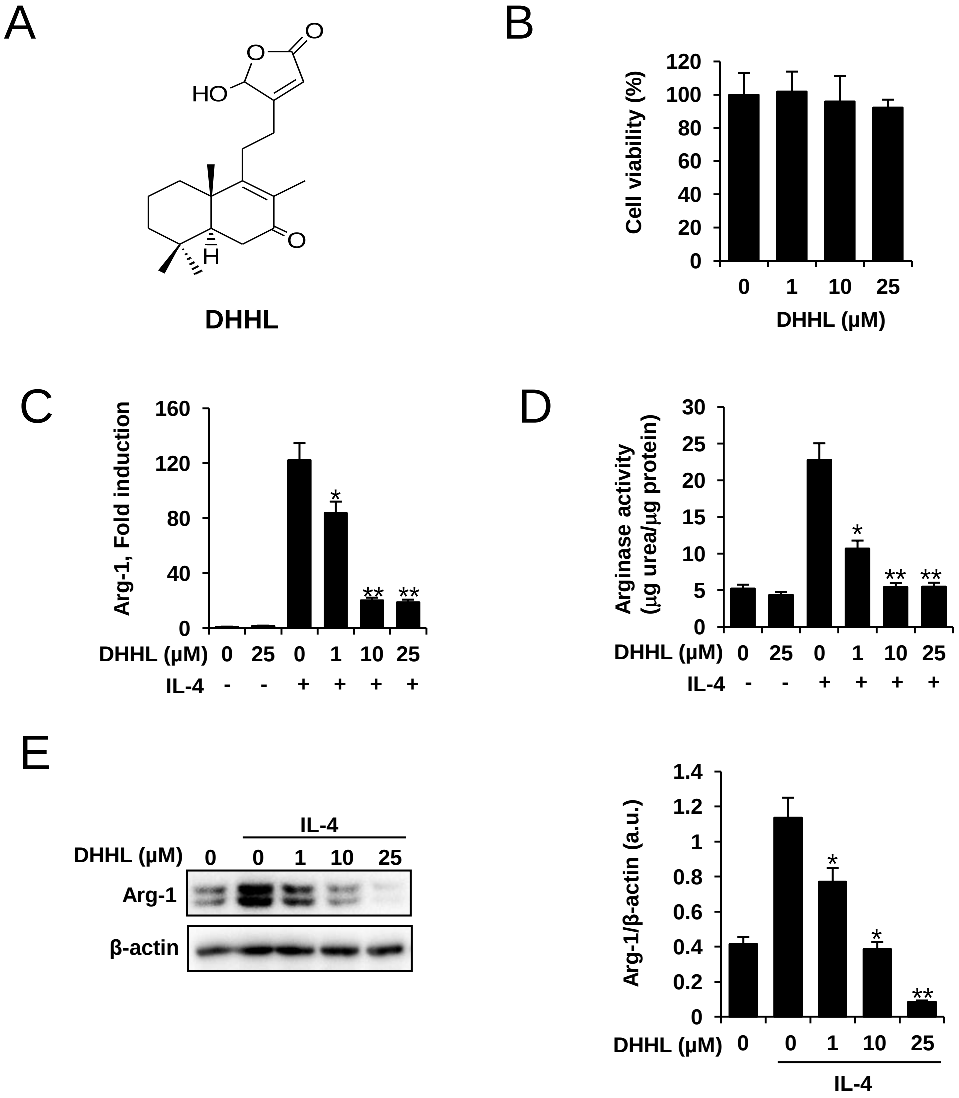

Jiménez-García et al., Figure 1

Figure 2

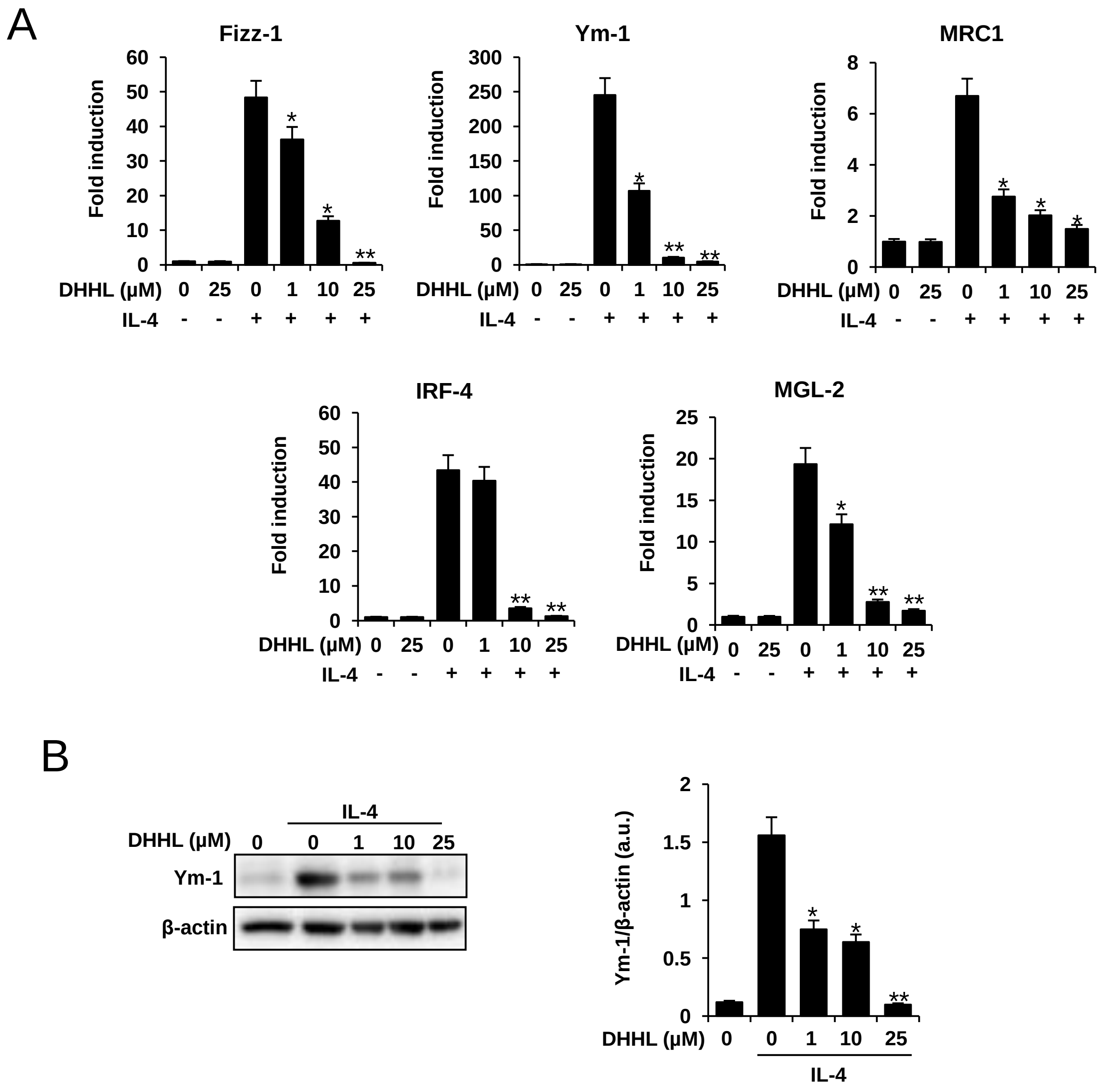

Jiménez-García et al., Figure 2

Figure 3

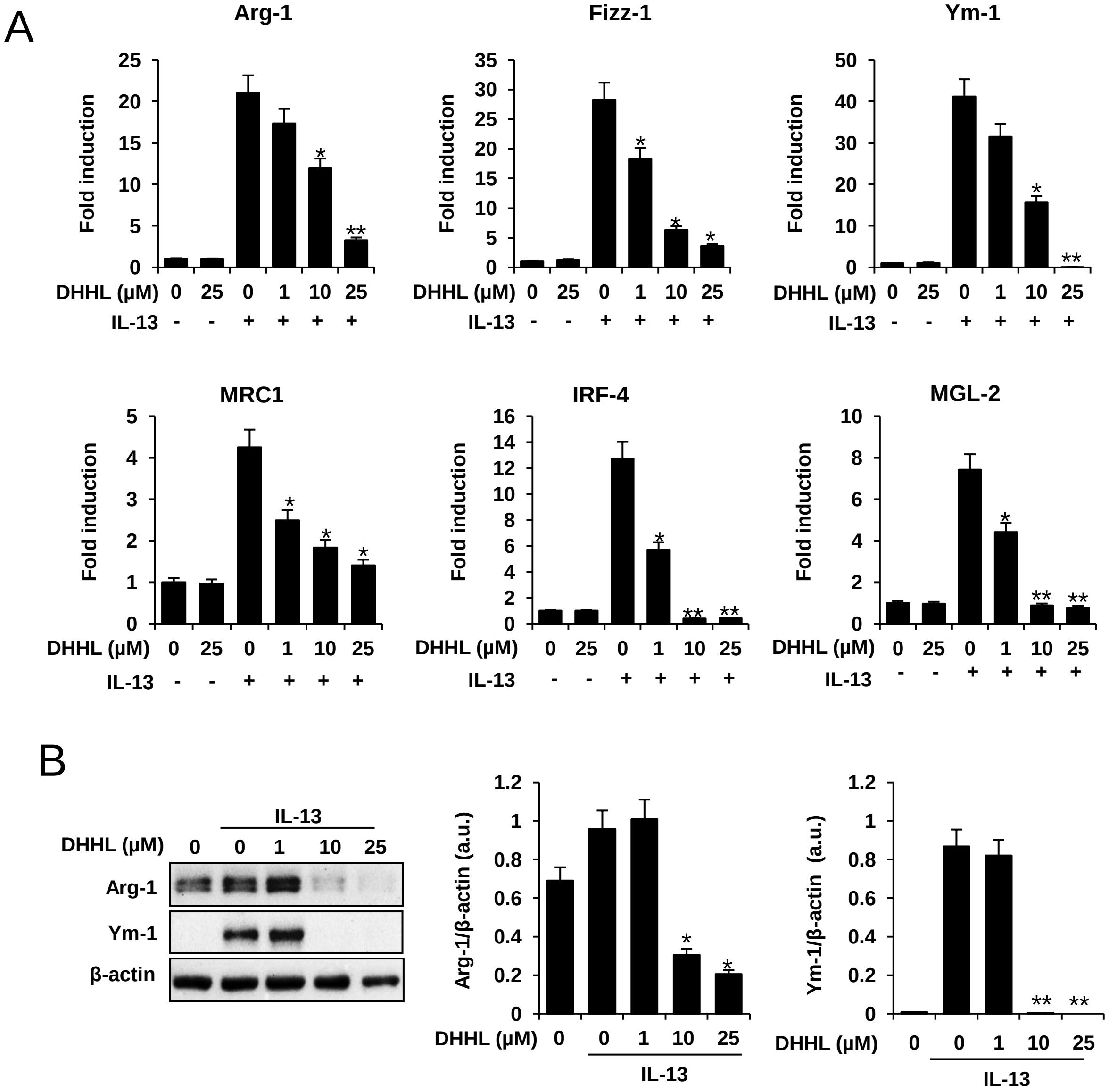

Jiménez-García et al., Figure 3

Figure 4

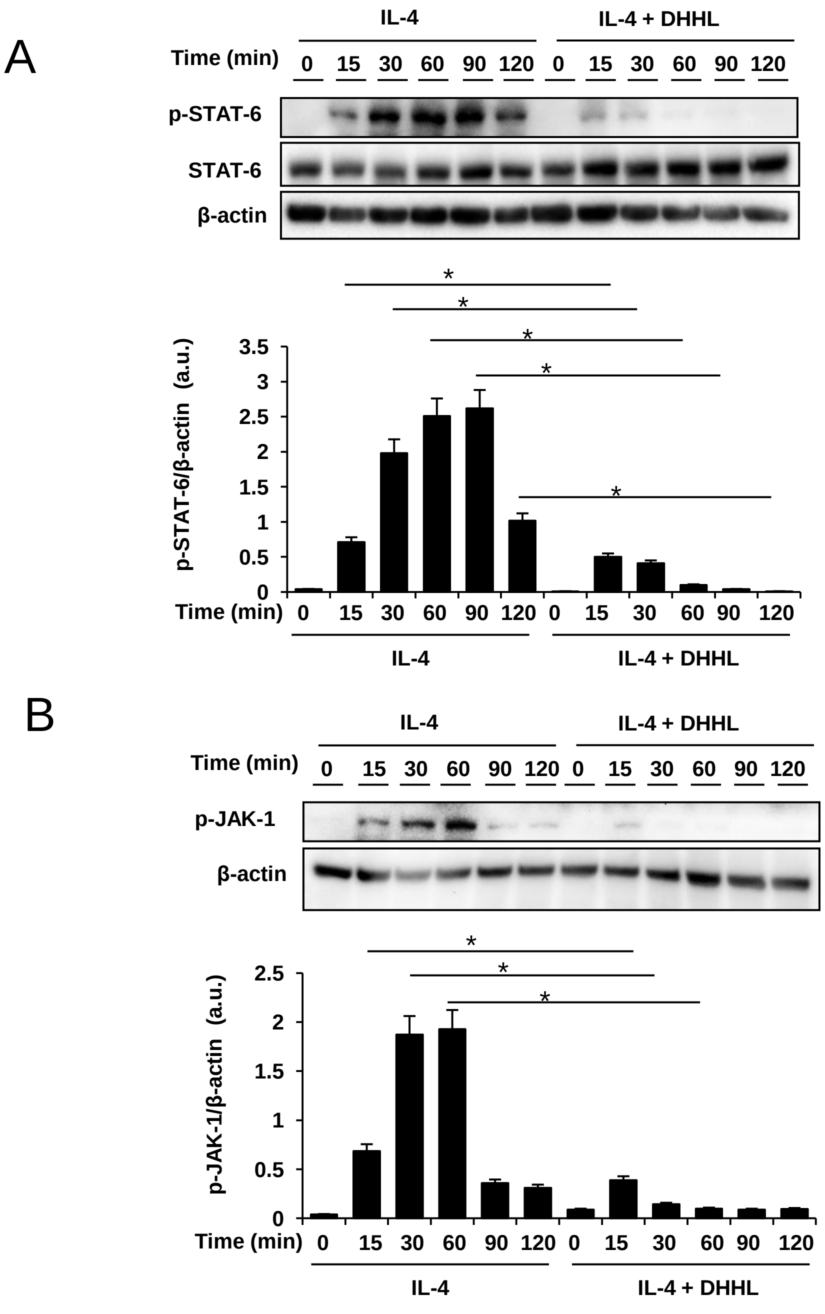

Jiménez-García et al., Figure 4

Figure 5

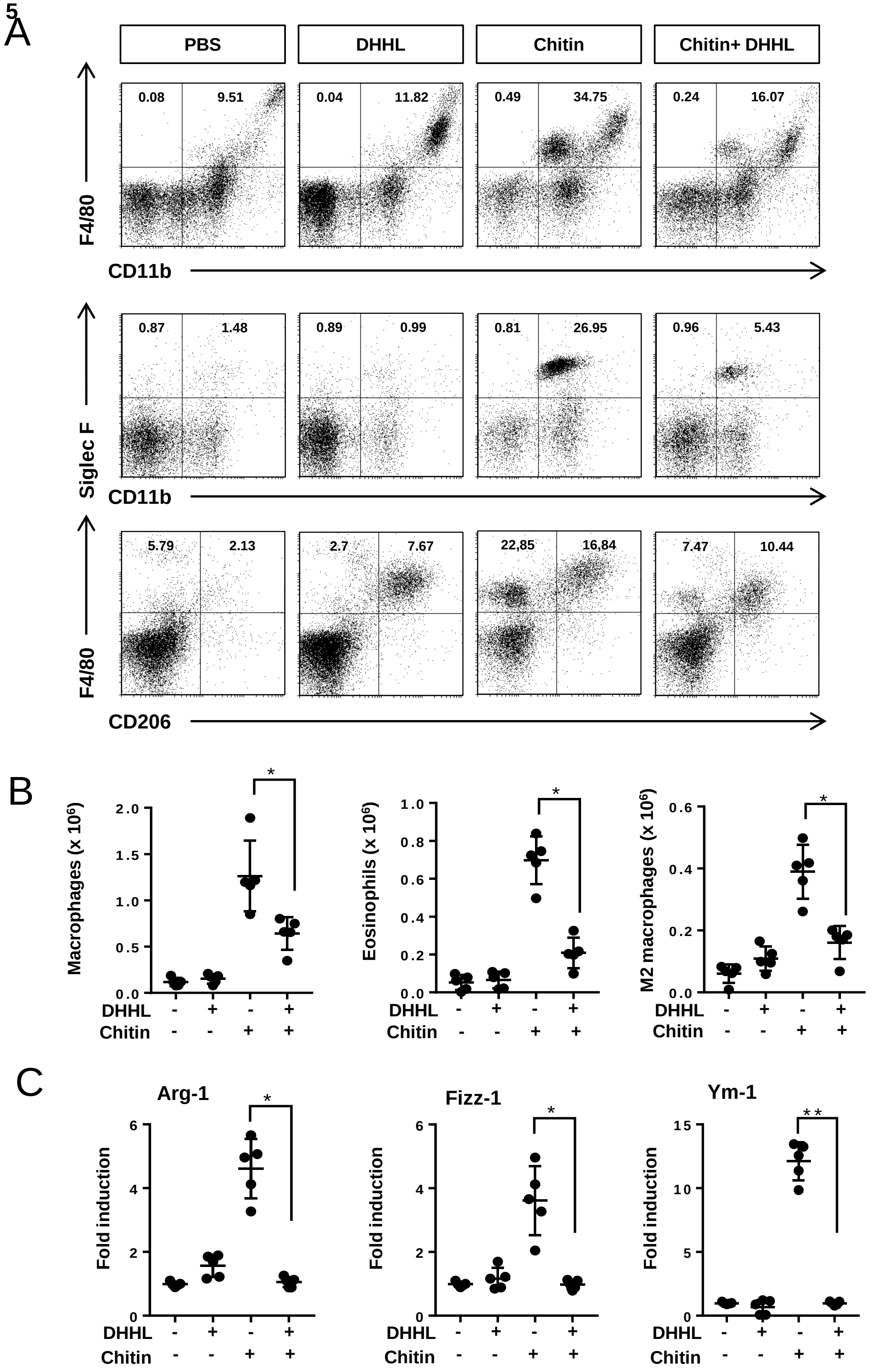

Jiménez-García et al., Figure 5

Figure 6

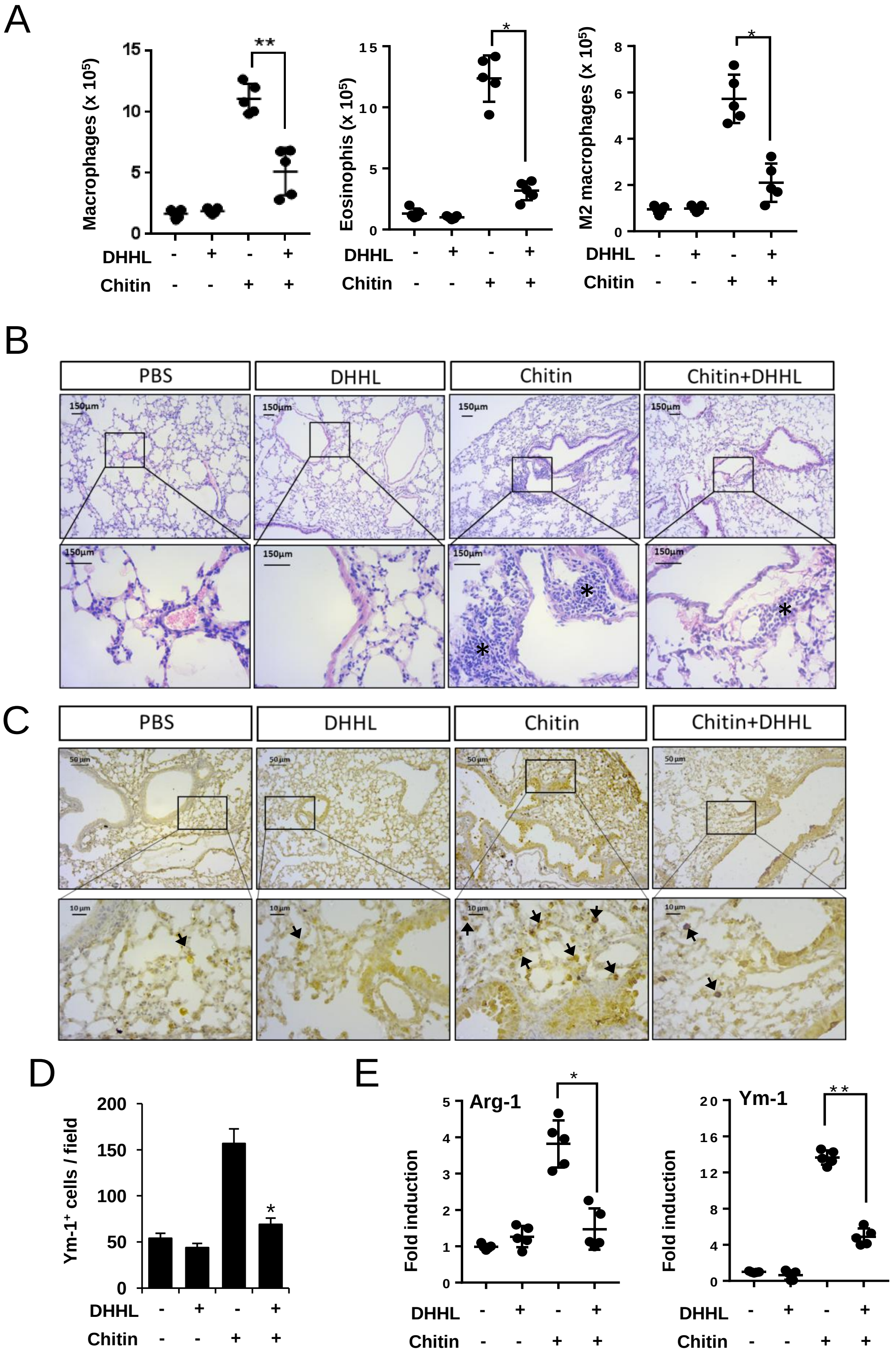

Jiménez-Garcia et al., figure 6.

Figure 7

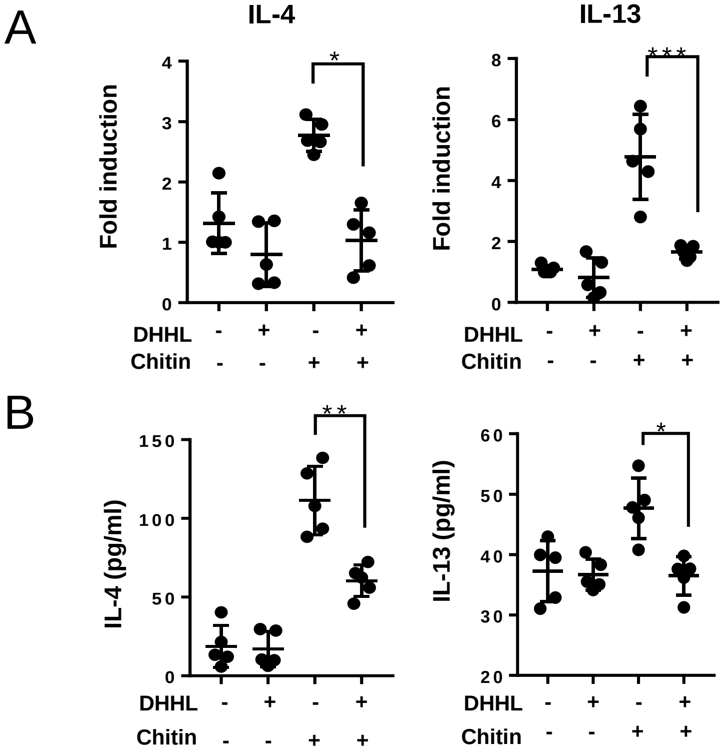

Jiménez-Garcia et al., figure 7.

Figure 8

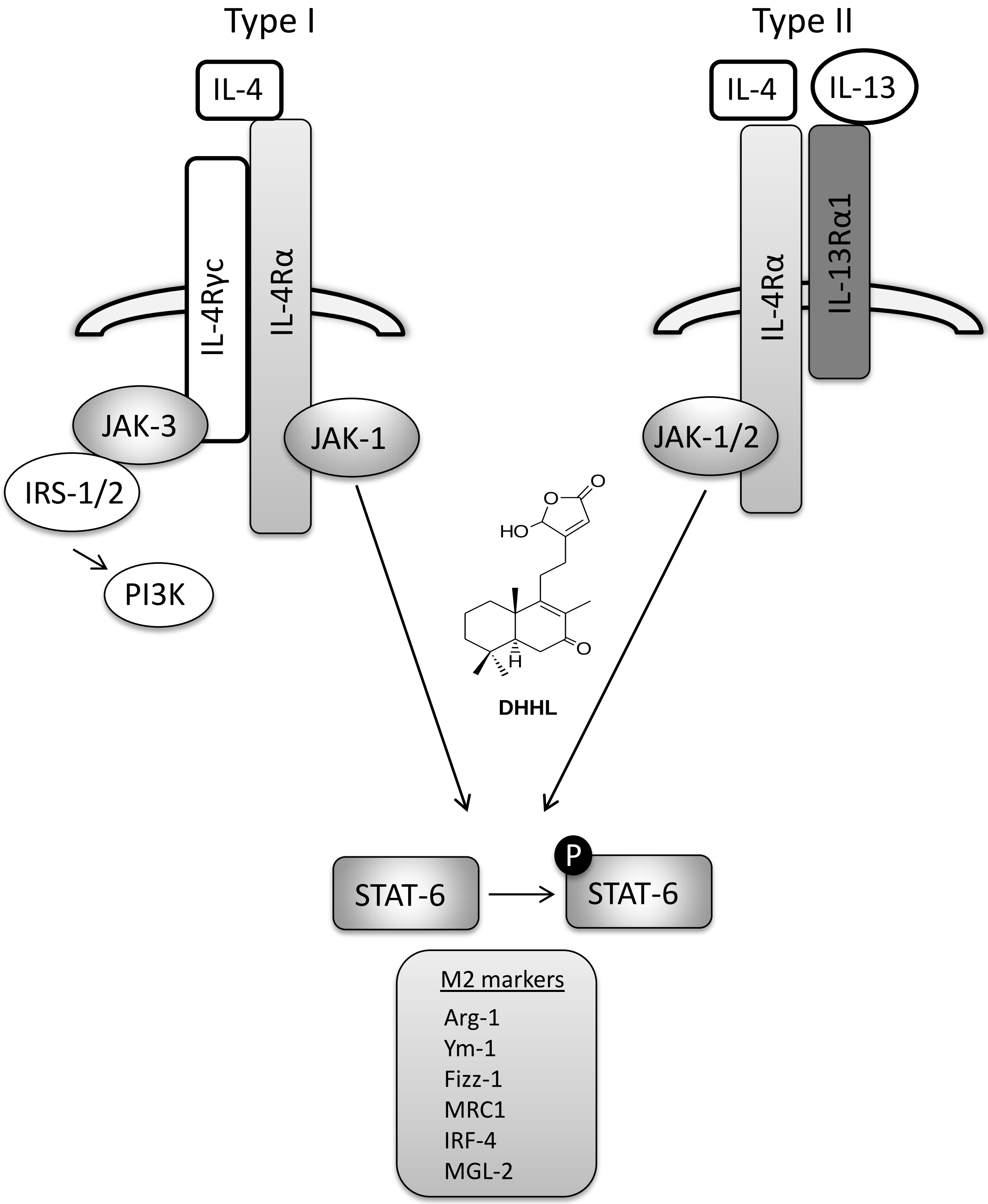

Jiménez-Garcia et al., figure 8.

Graphical Abstract (for review)

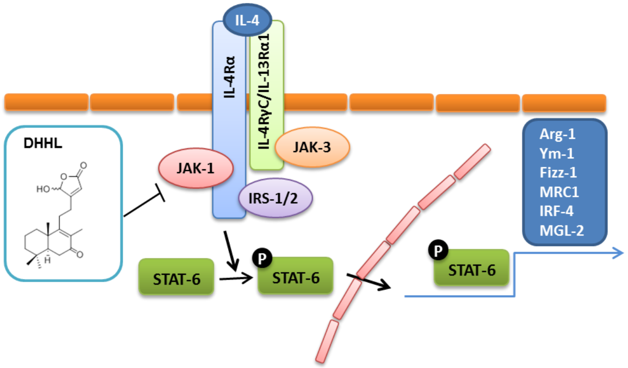

Jiménez-García et al.,